

Epstein–Barr virus-induced gene 3 negatively regulates neuroinflammation and T cell activation following coronavirus-induced encephalomyelitis

Emanuele Tirota^{a,1}, Patrick Duncker^{a,1}, Jean Oak^{a,2}, Suzi Klaus^a, Michelle R. Tsukamoto^a, Lanny Gov^a, Thomas E. Lane^{a,b,c,*}

^a Department of Molecular Biology and Biochemistry, University of California, Irvine 92697-3900, United States

^b Multiple Sclerosis Research Center, University of California, Irvine 92697-3900, United States

^c Sue and Bill Gross Stem Cell Center, University of California, Irvine 92697-3900, United States

ARTICLE INFO

Article history:

Received 5 September 2012

Received in revised form 9 October 2012

Accepted 9 October 2012

Keywords:

Virus

Cytokines

Neuroinflammation

Demyelination

ABSTRACT

Epstein–Barr virus-induced gene 3 (EBI3) associates with p28 and p35 to form the immunomodulatory cytokines IL-27 and IL-35, respectively. Infection of *EBI3*^{−/−} mice with the neuroadapted JHM strain of mouse hepatitis virus (JHMV) resulted in increased mortality that was not associated with impaired ability to control viral replication but enhanced T cell and macrophage infiltration into the CNS. IFN- γ secretion from virus-specific CD4⁺ and CD8⁺ T cells isolated from infected *EBI3*^{−/−} mice was augmented while IL-10 expression muted in comparison to infected WT mice. These data demonstrate a regulatory role for EBI3-associated cytokines in controlling host responses following CNS viral infection.

© 2012 Elsevier B.V. All rights reserved.

1. Introduction

Inoculation of the neurotropic JHM strain of mouse hepatitis virus (JHMV) into the CNS of susceptible strains of mice provides an excellent model in which to examine host response mechanisms responsible for both control of viral replication within distinct cell lineages present in the brain as well as host-derived factors regulating neuroinflammation (Bergmann et al., 2006). JHMV infection results in an acute encephalomyelitis characterized by wide-spread replication primarily in astrocytes and oligodendrocytes with relatively few neurons being infected (Knobler et al., 1981; Buchmeier and Lane, 1999; Parra et al., 1999; Perlman et al., 1999; Bergmann et al., 2006). Control of viral replication during acute disease relies on virus-specific CD8⁺ T cells, which function by two different effector mechanisms within the CNS: IFN- γ secretion is responsible for controlling viral replication in oligodendrocytes whereas a perforin-dependent mechanism promotes viral clearance from astrocytes (Lin et al., 1997; Parra et al., 1999). Infiltrating CD4⁺ T cells provide a supporting role for the maintenance and expansion of CTLs within

the CNS, as well as enhancing effector responses (Stohlman et al., 1998; Phares et al., 2012). Although a robust cell-mediated immune response occurs during acute disease, sterilizing immunity is not achieved, resulting in viral persistence (Stohlman and Weiner, 1981). Histological features associated with viral persistence include the development of an immune-mediated demyelinating disease with both T cells and macrophages being important in amplifying disease severity by contributing to myelin damage (Cheever et al., 1949; Perlman et al., 1999; Lane et al., 2000; Pewe and Perlman, 2002; Pewe et al., 2002).

EBV-induced gene-3 (EBI3) encodes a 34 kDa protein that is similar to the p40 subunit of IL-12 (Collison and Vignali, 2008; Wojno and Hunter, 2012). EBI3 is capable of binding subunits p28 or p35 (a subunit of IL-12) to form the cytokines IL-27 and IL-35, respectively (Collison and Vignali, 2008; Wojno and Hunter, 2012). Both IL-27 and IL-35 have important immunoregulatory roles controlling cytokine secretion and inflammation (Collison and Vignali, 2008; Yoshida and Miyazaki, 2008; Wojno and Hunter, 2012). Recent studies have highlighted that genetic ablation of EBI3 results in altered T cell-mediated cytokine expression (Yang et al., 2008) associated with increased inflammation as well as changes in the composition of the cellular infiltrate in experimental models of delayed-type hypersensitivity (Tong et al., 2010), autoimmune inflammation (Igawa et al., 2009; Liu et al., 2012), as well as hepatitis (Siebler et al., 2008). The influence of EBI3 in host defense in response to infection with a neurotropic virus has not been well characterized and was the focus of the present study.

* Corresponding author at: Department of Molecular Biology & Biochemistry, Multiple Sclerosis Research Center, University of California, Irvine 92697-3900, United States. Tel.: +1 949 824 5878; fax: +1 949 824 8551.

E-mail address: tlane@uci.edu (T.E. Lane).

¹ Equal contribution.

² Present address: Department of Pathology, Stanford University School of Medicine, Palo Alto, CA, United States.

2. Materials and methods

2.1. Virus and mice

EBI3^{-/-} mice (on the C57BL/6, H-2^b background) were generated as previously described (Yang et al., 2008) and generously provided by Centecor. Age-matched *EBI3*^{-/-} or C57BL/6 control mice (C57BL/6, H-2^b, National Cancer Institute, Frederick, MD) were used at 5–8 weeks of age for all experiments. For CNS infection studies, mice were intracranially (i.c.) injected with 250 plaque forming units (PFU) of MHV strain J2.2v-1 (JHNV) suspended in 30 μ L of sterile HBSS. Animals were sacrificed at defined time points and one-half of each brain at each time point was used for plaque assay on a mouse astrocytoma cell line (Hirano et al., 1978; Lane et al., 2000; Liu et al., 2000; Held et al., 2008). For systemic MHV infection, mice were intraperitoneally (i.p.) injected with 2.5×10^5 PFU of MHV strain DM suspended in 500 μ L HBSS. Control (sham) mice were injected with sterile HBSS alone. All experiments were approved by the University of California, Irvine Institutional Animal Care and Use Committee.

2.2. Flow cytometry

Mononuclear cells were obtained from tissues (brains and spleens) at defined times post-infection with JHNV using previously described methods (Lane et al., 2000; Stiles et al., 2006; Held et al., 2008). In brief, single cell suspensions of experimental tissues (all depleted of red blood cells) were stained with combinations of antibodies directed against the following surface markers: CD4, CD8a, CD44, CD25, CD62L, IA-IE (BD Biosciences), CD45 (eBiosciences), and F4/80 (Ab Direct). In all cases, isotype-matched control antibodies were used. Virus-specific CD4⁺ and CD8⁺ T cells recognizing their respective immunodominant epitope between amino acids 133 and 147 of the membrane (M) glycoprotein (M133–147) and surface (S) glycoprotein (S510–518) were determined by intracellular IFN- γ staining using previously described methods (Glass et al., 2002; Glass and Lane, 2003). The presence of virus-specific CD8⁺ T cells was also evaluated using S510–518 MHC class I tetramers as previously described (Stiles et al., 2006). Frequency data are presented as the percentage of positive cells within the gated population. Total cell numbers were calculated by multiplying these values by the total number of live cells isolated.

2.3. Quantitative real-time PCR

Total RNA from brains of experimental mice was extracted in Trizol (Invitrogen, Carlsbad, CA) and purified from infected *EBI3*^{-/-} and WT mice as well as sham-infected mice (Ambion). cDNA synthesis was performed using Superscript VILO cDNA Synthesis Kit (Invitrogen). Real-Time PCR analysis was completed using a LightCycler 480 Instrument II (Roche). IL-10 mRNA levels were assessed using specific primers: forward primer – AGCCGGAAGACAATAACTG; reverse primer – GGAGTCGGTTAGCAGTATGTTG. Amplicon expression was normalized to GAPDH (Invitrogen). LightCycler 480 SYBR Green I Master (Roche) was used in all reactions with the following assay conditions: 10 min initial denaturation at 95 °C, and 45 cycles of 30 s at 95 °C and 1 min at 60 °C. Data were analyzed using LightCycler 480 software (Roche).

2.4. Ex vivo cytokine production

C57BL/6 mice were injected via i.p. with 2.5×10^5 PFU of MHV strain DM suspended in 500 μ L HBSS. Mice were sacrificed at day 7 p.i. and splenocytes stimulated with 5 μ M OVA, M133, or S510 peptides for 48 h were collected and determined for IL-10 and IFN- γ secretion using the respective R&D DuoSet ELISA kits.

2.5. CTL assay

Spleen-derived CD8⁺ T cells were analyzed for lytic activity at day 7 following i.p. infection of WT and *EBI3*^{-/-} mice with 2.5×10^5 PFU of the DM strain of MHV. Numbers of S510–518-specific CD8⁺ T cells were determined by intracellular IFN- γ staining following exposure to the S510–518 peptide. CTL assays were performed with RMA-s (H-2^b) target cells preincubated with 5 μ M S510–518 peptide or OVA peptide as a control that were combined with immune CD8⁺ T cells at various effector:target ratios. Amounts of lactate dehydrogenase (LDH) released from lysed cells were determined by using a CytoTox 96® Non-Radioactive Cytotoxicity Assay (Promega, Madison, WI). Percentage lysis was determined as specified by manufacturer's protocols. Percentage lysis of OVA peptide-pulsed co-cultures was subtracted from the percentage lysis of S510–518 pulsed co-cultures to eliminate background CTL activity.

2.6. Histology and immunohistochemistry

Brains and spinal cords from experimental mice were harvested from PBS-perfused mice and fixed in 4% paraformaldehyde overnight. Brain tissues were embedded in paraffin and stained with hematoxylin and eosin (H&E). Spinal cords were fixed in normal balance formalin for 24 h and then embedded in paraffin. Sections of spinal cords were stained with luxol fast blue (LFB) to identify myelin (blue) and counterstained with Harrison hematoxylin and eosin to visualize cellular inflammation (Lane et al., 2000; Liu et al., 2001). Rabbit anti-mouse GFAP (Invitrogen, Carlsbad, CA) (1:500 dilution in phosphate-buffered saline containing 10% normal rabbit serum [NRS]) used for detection of activated astrocytes. A biotinylated secondary antibody (1:400 dilution, Vector Laboratories, Burlingame, CA) was used for detection. Staining was performed on 6 μ m-thick frozen sections fixed with 4% paraformaldehyde. The ABC Elite (Vector Laboratories) staining system was used according to the manufacturer's instructions, and diaminobenzidine (DAB) was used as a chromogen. All slides were counterstained with hematoxylin, dehydrated, and mounted. Staining controls were (i) omission of primary antibodies from the staining sequence and (ii) treatment of sham-infected mice with primary and secondary antibodies.

2.7. Statistical analysis

2-Tailed unpaired Student's *T*-test was conducted to determine statistical significance for all assays.

3. Results

3.1. Survival and histopathology

Wildtype (WT) and *EBI3*^{-/-} mice were infected intracranially (i.c.) with 250 PFU of JHNV to evaluate the contributions of *EBI3* in host defense. Genetic ablation of *EBI3* signaling was associated with increased ($p \leq 0.01$) susceptibility to JHNV-induced death with ~70% of infected *EBI3*^{-/-} mice dying by day 12 p.i. whereas only ~30% of WT mice died (Fig. 1A). Examination of brains of JHNV-infected mice revealed that *EBI3*^{-/-} mice displayed overall increased thickening of the meninges as well as increased perivascular cuffing when compared to infected WT mice indicating enhanced neuroinflammation in response to JHNV infection in the absence of *EBI3* expression (Fig. 1B). Additionally, increased astrogliosis, as determined by GFAP staining, was evident in JHNV-infected *EBI3*^{-/-} mice in comparison to WT mice (Fig. 1C).

3.2. CNS viral titers and neuroinflammation

To determine if increased death was the result of an inability to control viral replication, viral titers within the brains of infected WT and

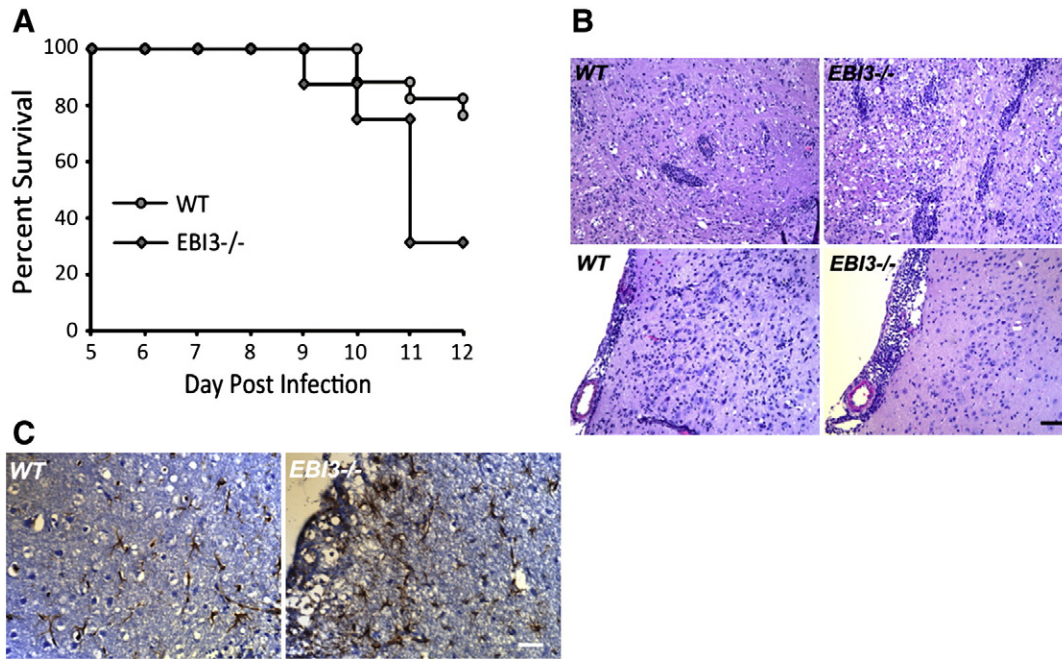


Fig. 1. Mortality and neuroinflammation following JHMV infection of the CNS. (A) WT and *EB13*^{-/-} mice were infected i.c. with 250 PFU of JHMV and survival determined. Data presented is representative of 3 independent experiments with a minimum of 6 mice/experiment. (B) Representative H&E staining showing increased perivascular cuffing (top panels) and increased meningeal inflammation in the brains of JHMV-infected WT and *EB13*^{-/-} mice at day 7 p.i. (C) Representative GFAP staining showing increased astrogliosis within the brains of JHMV-infected *EB13*^{-/-} mice compared to WT mice at day 7 p.i.

EB13^{-/-} mice were determined. As shown in Fig. 2A, similar viral titers were present within the brains of both WT and *EB13*^{-/-} mice at day 5 p.i. By day 7 p.i., *EB13*^{-/-} mice displayed elevated titers ($p \leq 0.05$) compared to WT mice yet both groups of mice reduced titers below the level of detection (~ 100 PFU/g tissue) at day 12 p.i. Flow analysis of T cell infiltration into the CNS of infected animals revealed reduced ($p \leq 0.05$) numbers of CD4⁺ and CD8⁺ T cells present within the brains of infected *EB13*^{-/-} mice compared to WT mice at day 5 p.i. (Fig. 2B). However, by day 7 p.i., there were increased numbers of CD8⁺ T cells present in the CNS of infected *EB13*^{-/-} mice compared to WT mice and this was sustained out to day 12 p.i. (Fig. 2B). In contrast, there were no differences in numbers of inflammatory CD4⁺ T cells within the CNS of infected WT and *EB13*^{-/-} mice at days 7 and 12 p.i. (Fig. 2B). Further examination revealed enhanced activation (CD62L⁻CD25⁺) states in both CD4⁺ and CD8⁺ T cell (Fig. 2C) subsets present within the CNS of JHMV-infected *EB13*^{-/-} mice compared to WT mice. Macrophage (CD45^{high}F4/80⁺) infiltration, as determined by flow cytometric analysis, was elevated in infected *EB13*^{-/-} mice at days 7 ($p \leq 0.05$) and 12 p.i. ($p \leq 0.01$) when compared to infected WT mice (Fig. 3A). In addition, flow analysis revealed increased ($p \leq 0.05$) MHC class II expression on activated microglia at days 7 and 12 p.i. suggesting increased IFN- γ levels within the CNS of JHMV-infected *EB13*^{-/-} mice when compared to infected WT mice (Fig. 3B). Earlier studies indicate that the absence of EB13 alters the immunomodulatory cytokine IL-10 levels in models of inflammation (Zahn et al., 2005; Hausding et al., 2007; Tong et al., 2010). In accordance with these earlier studies, we detected significantly ($p \leq 0.01$) lower levels of mRNA transcripts specific for IL-10 within the brains of infected *EB13*^{-/-} mice compared to WT mice (Fig. 3C). Evaluation of demyelination revealed comparable levels of white matter damage in both infected *EB13*^{-/-} and WT mice (Fig. 3D).

3.3. Virus-specific T cells

Intracellular IFN- γ staining in response to defined CD4 [Matrix (M) protein spanning epitopes 133–144] and CD8 [Spike (S) glycoprotein

spanning epitopes 510–518] viral epitopes was employed to measure infiltration of virus-specific T cells into the CNS of JHMV-infected mice. Analysis at day 7 p.i. revealed reduced ($p < 0.05$) numbers of M133–144-specific CD4⁺ T cells in the brains of infected *EB13*^{-/-} mice compared to WT mice while infiltration of S510–518-specific CD8⁺ T cells was significantly ($p < 0.05$) increased in *EB13*^{-/-} mice compared to WT mice (Fig. 4A and B). S510–518 MHC class I tetramer staining confirmed increased numbers ($p \leq 0.05$) of virus-specific CD8⁺ T cells within the CNS of *EB13*^{-/-} mice when compared to WT mice (Fig. 4C). By day 12 p.i., there were increased ($p \leq 0.001$) numbers of virus-specific CD4⁺ and CD8⁺ T cells present in the brains of *EB13*^{-/-} mice compared to WT mice (not shown). To determine if CTL activity was influenced by loss of EB13 expression, ex vivo CTL assays were performed. WT and *EB13*^{-/-} mice were infected i.p. with MHV and spleens were removed at day 7 p.i. Similar frequencies of virus-specific CD8⁺ T cells were present within the spleens of infected WT and *EB13*^{-/-} mice as determined by intracellular IFN- γ staining in response to S510–518 as well as S510–518 MHC class I tetramer staining (not shown). As shown in Fig. 4D, CTL activity is slightly muted at all E:T ratios tested arguing for a potential role for EB13 in augmenting CTL activity.

3.4. T cell cytokine production

We next interrogated how genetic ablation of EB13 influenced T cell responses following JHMV infection. Both WT and *EB13*^{-/-} mice were challenged by i.p. injection with virus and splenocytes isolated at day 7 p.i. Intracellular IFN- γ staining demonstrated decreased ($p \leq 0.05$) numbers of M133–147-specific CD4⁺ T cells isolated from the spleens of *EB13*^{-/-} mice compared to WT mice while comparable numbers of S510–518-positive CD8⁺ T cells were present in both WT and *EB13*^{-/-} mice (Fig. 5A). Cultured T cells were stimulated with either M133–147 or S510–518 and IFN- γ levels determined by ELISA. As shown in Fig. 5B, T cells from *EB13*^{-/-} mice produced significantly more IFN- γ in response to peptide stimulation in comparison to WT mice. There was a ~ 2 -fold increase ($p \leq 0.05$) in IFN- γ

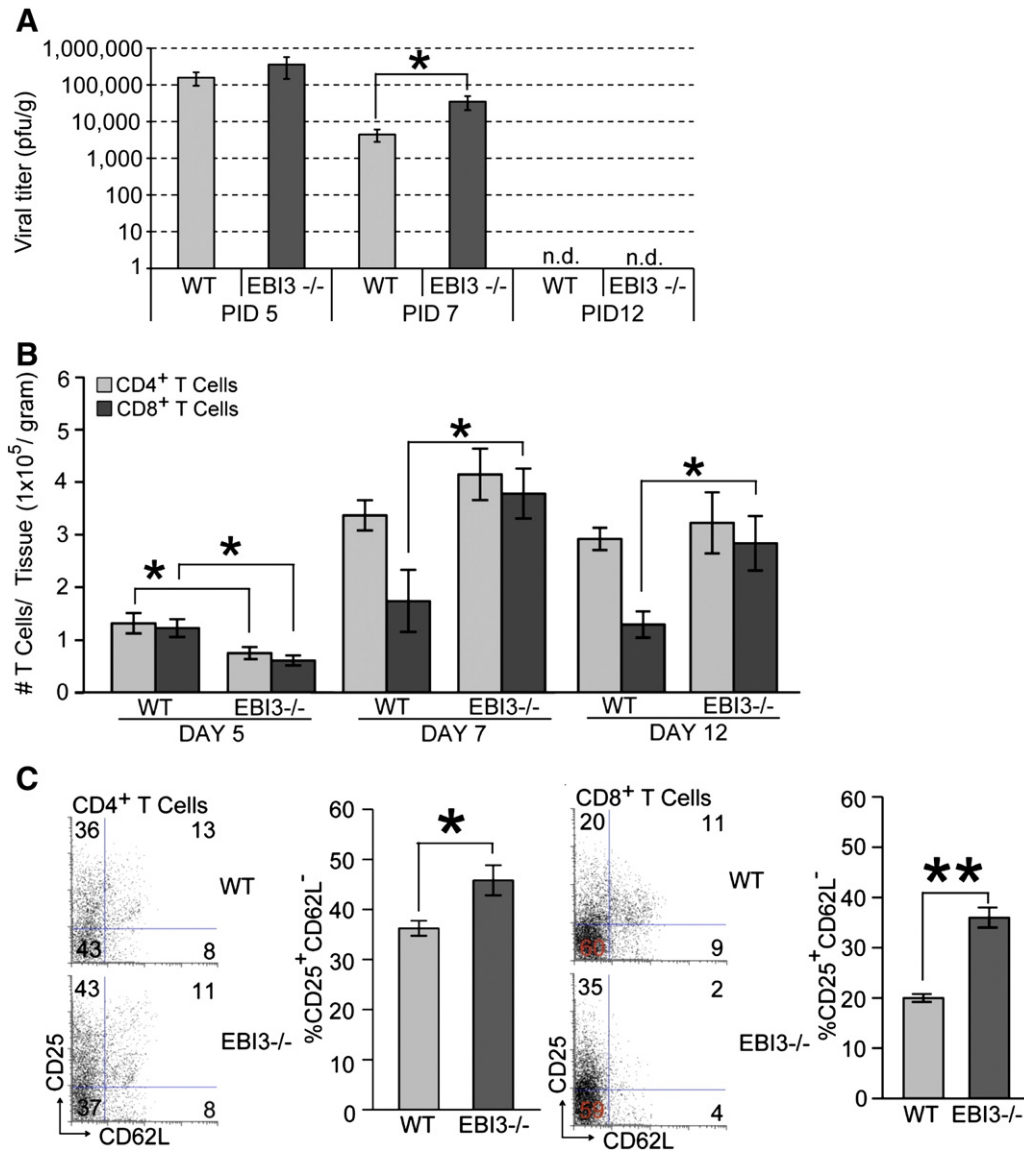


Fig. 2. Brain viral titers and T cell infiltration. (A) WT and *EB13*^{-/-} mice were i.c. infected with 250 PFU of JHMV and viral titers determined at days 5, 7, and 12 p.i. (B) T cell infiltration into the CNS of JHMV-infected mice was determined by flow cytometry at days 5, 7, and 12 p.i. (C) Activation status of T cells was determined by measuring CD62L and CD25 expression on T cells infiltrating into the CNS of JHMV-infected mice by flow cytometry. Representative dot blots are shown for CD4⁺ T cells and CD8⁺ T cells; and the overall increase in CD62L^{lo}CD25^{hi} CD4⁺ and CD8⁺ T cell subsets in infected *EB13*^{-/-} mice compared to WT mice is shown. For all experiments, data is representative of 2 independent experiments with a minimum of 3 mice per time point; data is presented as average ± SEM; * indicates p ≤ 0.05.

production by M133–147-specific CD4⁺ T cells from *EB13*^{-/-} mice while IFN-γ levels were increased >2.5-fold (p ≤ 0.01) by S510–518-specific CD8⁺ T cells isolated from *EB13*^{-/-} mice. In addition, IL-10 production was significantly (p ≤ 0.05) reduced in antigen-stimulated virus-specific *EB13*^{-/-} T cells compared to WT cells (Fig. 5C).

4. Discussion

In this study, we demonstrate that *EB13* plays an important role in controlling neuroinflammation and T cell responses in response to JHMV infection of the CNS. Specifically, JHMV infection of *EB13*-deficient mice increased mortality during the acute stage of the disease and this is not the result of impaired ability to control viral replication. Rather, increased disease severity was associated with enhanced leukocyte entry into the CNS with greater numbers of both CD8⁺ T cells and virus-specific CD8⁺ T cells when compared to WT mice. In addition, IFN-γ secretion was increased following viral peptide stimulation of *EB13*-deficient CD4⁺ and CD8⁺ T cells isolated from JHMV-infected

mice. Although IFN-γ production was elevated in CD8⁺ T cells, CTL activity was muted indicating differential roles for *EB13* in contributing to antiviral effector functions. These findings highlight that within the context of JHMV infection of the CNS, *EB13* is important in influencing virus-specific CD8⁺ T cell effector function yet the overall impact of how this contributes to increased mortality remains enigmatic and requires continued investigation.

Previous studies indicate that genetic ablation of *EB13* influences cytokine production by T cells. For example, delayed-type hypersensitivity is dramatically exacerbated in *EB13*^{-/-} associated with enhanced infiltration of inflammatory cells into the footpad of antigen-challenged mice as compared to control animals (Tong et al., 2010). In addition, *EB13* negatively regulates T cell production of IL-17 and IL-22 and this correlated with enhanced expression of the transcription factor RORγT (Yang et al., 2008). Experimental infection of *EB13*-deficient mice with *Leishmania* demonstrated muted Th1 responses indicating a potential role in regulating immune responses following microbial infection (Zahn et al., 2005). The majority of

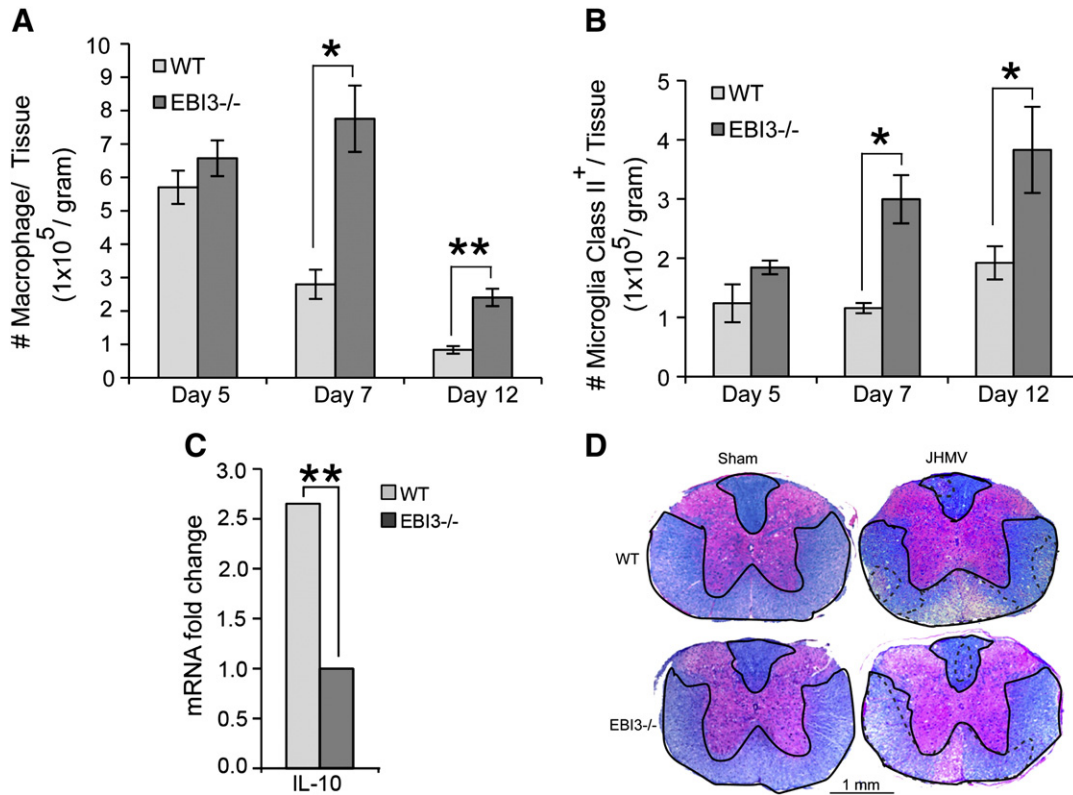


Fig. 3. Macrophage infiltration and demyelination. (A) Macrophage (CD45^{high}F480⁺) infiltration into the CNS of infected mice was determined at days 5, 7, and 12 p.i. by flow cytometry. (B) MHC class II expression on resident microglia (CD45^{lo}F480⁺) from infected EB13^{-/-} and WT mice was determined at days 5, 7, and 12 p.i. by flow cytometry. Data for A and B is derived from 2 independent experiments with a minimum of 3 mice per time point; data is presented as average + SEM and * indicates $p \leq 0.05$. (C) Expression of mRNA transcripts specific for IL-10 within the brains of JHMV-infected EB13^{-/-} and WT mice at day 7 p.i. was performed by qPCR analysis. Data is derived from 4 mice from each experimental group and presented as average \pm SEM fold change compared to sham-infected mice; ** indicates $p \leq 0.01$. (D) Representative spinal cord sections from JHMV-infected EB13^{-/-} and WT mice isolated at day 12 p.i. and stained with luxol fast blue to assess the severity of demyelination (areas of white matter pathology are outlined by hashmarks).

studies examining the importance of EB13 in tailoring T cell responses have characterized a role within the context of IL-27 (EB13/p28) signaling. These studies have highlighted an important role for IL-27 in modulating T cell as well as inflammatory responses. IL-27 signals through a heterodimeric receptor consisting of IL-27Ra (WX1) and gp130 (Pflanz et al., 2004). Originally characterized as a proinflammatory cytokine that was necessary for initiation of Th1 differentiation (Pflanz et al., 2002), IL-27 expression was shown to be critical in generation of protective T cell responses in response to infection with *Leishmania major* (Zahn et al., 2005). However, additional studies have shown that loss of IL-27 signaling through genetic ablation of either EB13 or IL27Ra does not diminish the ability to generate a protective Th1 response (Batten and Ghilardi, 2007). Rather, animals lacking these genes have exhibited enhanced immune responses associated with accelerated tissue damage that correlates with elevated levels of proinflammatory cytokines including IFN- γ following infection with *Toxoplasma gondii* and *Mycobacterium tuberculosis* (Villarino et al., 2003; Holscher et al., 2005). With regard to viral infection, IL-27 has been shown to exert an anti-viral effect on HIV and evidence suggests that this is mediated, in part, by activating multiple interferon-inducible genes (Fakruddin et al., 2007; Imamichi et al., 2008).

Whether increased neuroinflammation and IFN- γ secretion by T cells in response to JHMV infection of the CNS is due to impaired signaling through either IL-27 or IL-35 remains to be determined. However, a recent study by Liu et al. (2012) examined the influence of EB13 within the context of experimental autoimmune encephalomyelitis (EAE), an autoimmune model of neuroinflammation and demyelination. Similar to our findings, there was increased neuroinflammation in MOG-immunized EB13^{-/-} mice compared to WT controls and this was

accompanied by increased Th1 responses (Liu et al., 2012). However, production of IFN- γ was not affected in EB13^{-/-} mice but IL-2 and IL-17 levels were dramatically elevated. Although neuroinflammation was increased in EB13^{-/-} mice with EAE, the severity of disease was only marginally enhanced compared to WT mice and this may be the result of increased numbers of CD4⁺Foxp3⁺Treg's that exhibited potent suppressive functions (Liu et al., 2012). IL-17-producing T cells are not detected within the CNS of JHMV-infected mice so it is unlikely that the absence of EB13 affects secretion of IL-17 in this model (Held et al., 2008; Kapil et al., 2009). Whether Tregs are increased in number and/or exhibit enhanced suppressor functions in response to JHMV infection of EB13^{-/-} mice is unknown at this time. It is interesting to speculate that a reason that the severity of demyelination is not dramatically increased in JHMV-infected EB13^{-/-} mice compared to WT mice even in the face of increased neuroinflammation may be the result of enhanced suppressor activity by Tregs and this is currently under investigation.

Our findings that EB13 deficiency increases IFN- γ secretion are consistent with other studies examining how EB13/IL-27 controls T cell responses following microbial infection (Villarino et al., 2003; Stumhofer et al., 2006). Moreover, a recent study by Stumhofer et al. (2006) has demonstrated enhanced anti-tumor responses by CD8⁺T cells in EB13^{-/-} mice associated with increased IFN- γ production. Therefore, loss of EB13 expression is not restricted to altered effector functions in CD4⁺T cell subsets but can also include CD8⁺T cell subsets. An important question that remains to be resolved is whether the change in disease course and T cell responses in JHMV-infected EB13^{-/-} mice reflects deficiencies in IL-27 or IL-35 expression.

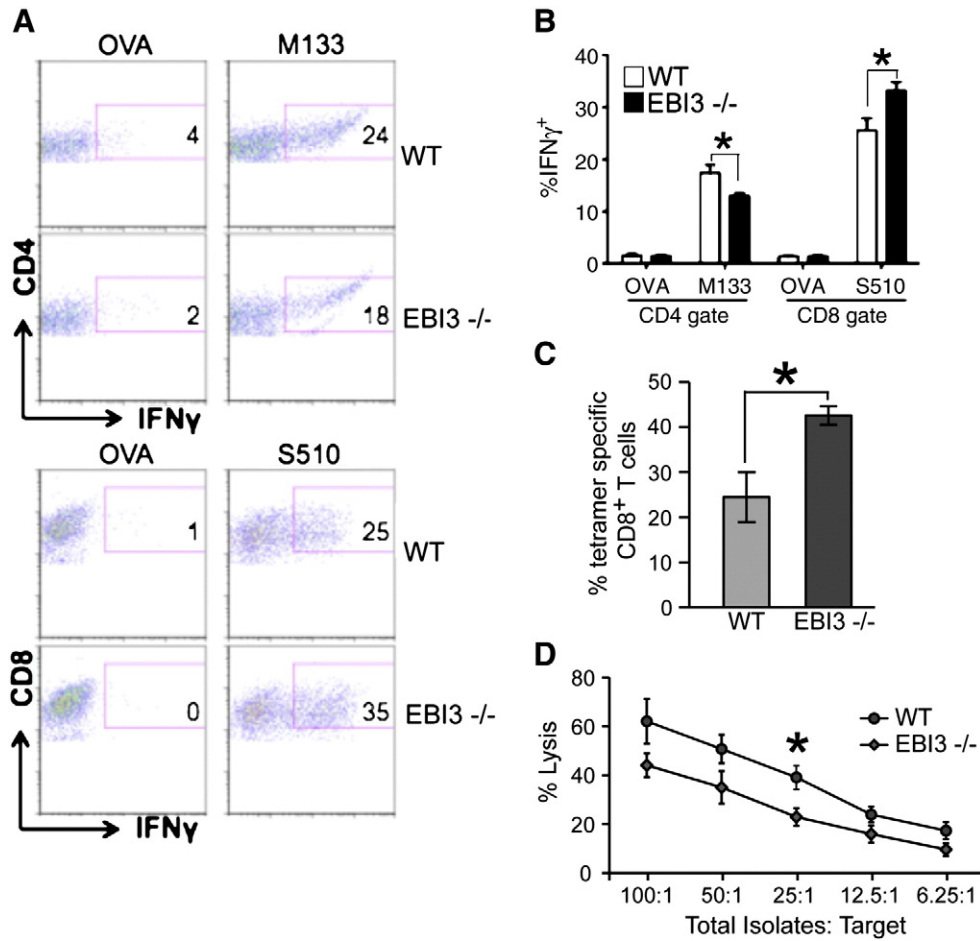


Fig. 4. Anti-viral T cell responses. WT and *EB13*^{-/-} mice were i.c. infected with 250 PFU of JHMV and generation of virus-specific T cells measured by intracellular IFN- γ staining in response to the CD4⁺ T cell epitope M133–147 and CD8⁺ T cell epitope S510–518. As controls, ovalbumin (OVA) peptides corresponding to defined CD4⁺ and CD8⁺ T cell subsets were also included. (A) Representative dot blots showing increased IFN- γ staining in CD4⁺ and CD8⁺ T cell subsets in infected *EB13*^{-/-} mice compared to WT mice at day 7 p.i. (B) Quantification of intracellular IFN- γ expression in response to viral peptides reveals increased frequencies of virus-specific CD4⁺ and CD8⁺ T cells within the brains of JHMV-infected *EB13*^{-/-} mice compared to WT mice. (C) Staining with the S510–518-MHC class I tetramer reveals increased staining within the brains of infected *EB13*^{-/-} mice compared to WT mice at day 7 p.i. Data in B and C is derived from 2 independent experiments with a minimum of 3 mice per group and presented as average \pm SEM; * indicates $p < 0.05$ (D) WT and *EB13*^{-/-} mice were infected i.p. with JHMV and splenocytes removed at day 7 p.i. CTL activity to S510–518-pulsed target cells was performed as previously described (Stiles et al., 2006) using different E:T ratios and * indicates $p \leq 0.05$.

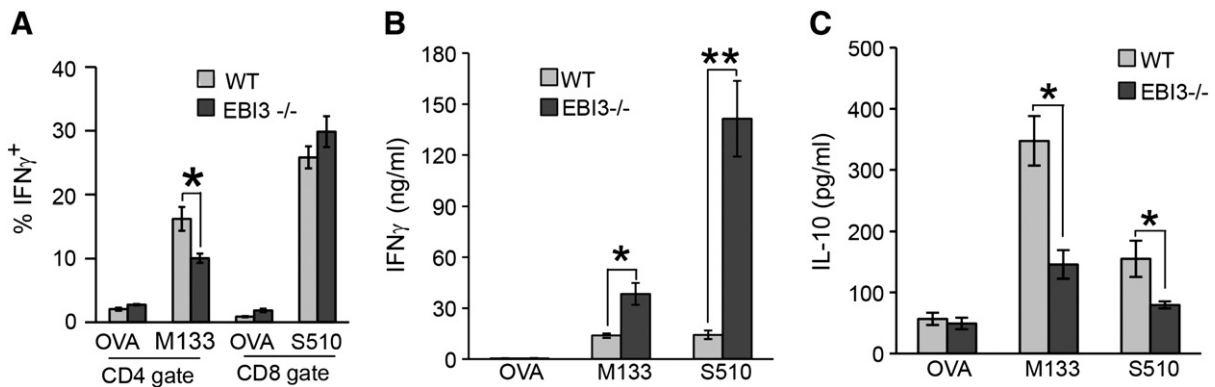


Fig. 5. T cell cytokine production. WT and *EB13*^{-/-} mice were injected i.p. with JHMV and splenocytes isolated at day 7 p.i. to evaluate expression of IFN- γ and IL-10 in response to viral peptide stimulation. (A) Intracellular IFN- γ staining reveals diminished frequency of M133–147-specific CD4⁺ T cells in *EB13*^{-/-} mice compared to WT whereas there were similar frequencies of virus-specific CD8⁺ T cells. Splenocytes from infected WT and *EB13*^{-/-} mice were stimulated with either 5 μ M M133–147 or S510–518 peptides for 48 h and secretion of IFN- γ (B) or IL-10 (C) determined by ELISA. * indicates $p \leq 0.05$ and ** indicates $p \leq 0.01$.

References

- Batten, M., Ghilardi, N., 2007. The biology and therapeutic potential of interleukin 27. *J. Mol. Med. (Berl.)* 85, 661–672.
- Bergmann, C.C., Lane, T.E., Stohlman, S.A., 2006. Coronavirus infection of the central nervous system: host-virus stand-off. *Nat. Rev. Microbiol.* 4, 121–132.
- Buchmeier, M.J., Lane, T.E., 1999. Viral-induced neurodegenerative disease. *Curr. Opin. Microbiol.* 2, 398–402.
- Cheever, F.S., Daniels, J.B., Pappenheimer, A.M., Bailey, O.T., 1949. A murine virus (JHM) causing disseminated encephalomyelitis with extensive destruction of myelin. *J. Exp. Med.* 90, 181–194.
- Collison, L.W., Vignali, D.A., 2008. Interleukin-35: odd one out or part of the family? *Immunol. Rev.* 226, 248–262.
- Fakruddin, J.M., Lempicki, R.A., Gorelick, R.J., Yang, J., Adelsberger, J.W., Garcia-Pineres, A.J., Pinto, L.A., Lane, H.C., Imamichi, T., 2007. Noninfectious papilloma virus-like particles inhibit HIV-1 replication: implications for immune control of HIV-1 infection by IL-27. *Blood* 109, 1841–1849.
- Glass, W.G., Lane, T.E., 2003. Functional analysis of the CC chemokine receptor 5 (CCR5) on virus-specific CD8+ T cells following coronavirus infection of the central nervous system. *Virology* 312, 407–414.
- Glass, W.G., Chen, B.P., Liu, M.T., Lane, T.E., 2002. Mouse hepatitis virus infection of the central nervous system: chemokine-mediated regulation of host defense and disease. *Viral Immunol.* 15, 261–272.
- Hausding, M., Karwot, R., Scholtes, P., Lehr, H.A., Wegmann, M., Renz, H., Galle, P.R., Birkenbach, M., Neurath, M.F., Blumberg, R.S., Finotto, S., 2007. Lung CD11c+ cells from mice deficient in Epstein-Barr virus-induced gene 3 (EBI-3) prevent airway hyper-responsiveness in experimental asthma. *Eur. J. Immunol.* 37, 1663–1677.
- Held, K.S., Glass, W.G., Orlovsky, Y.I., Shamberger, K.A., Petley, T.D., Branigan, P.J., Carton, J.M., Beck, H.S., Cunningham, M.R., Benson, J.M., Lane, T.E., 2008. Generation of a protective T-cell response following coronavirus infection of the central nervous system is not dependent on IL-12/23 signaling. *Viral Immunol.* 21, 173–188.
- Hirano, N., Murakami, T., Fujiwara, K., Matsumoto, M., 1978. Utility of mouse cell line DBT for propagation and assay of mouse hepatitis virus. *Jpn. J. Exp. Med.* 48, 71–75.
- Holscher, C., Holscher, A., Ruckerl, D., Yoshimoto, T., Yoshida, H., Mak, T., Saris, C., Ehlers, S., 2005. The IL-27 receptor chain WSX-1 differentially regulates antibacterial immunity and survival during experimental tuberculosis. *J. Immunol.* 174, 3534–3544.
- Igawa, T., Nakashima, H., Sadanaga, A., Masutani, K., Miyake, K., Shimizu, S., Takeda, A., Hamano, S., Yoshida, H., 2009. Deficiency in EBV-induced gene 3 (EBI3) in MRL/lpr mice results in pathological alteration of autoimmune glomerulonephritis and sialadenitis. *Mod. Rheumatol.* 19, 33–41.
- Imamichi, T., Yang, J., Huang, D.W., Brann, T.W., Fullmer, B.A., Adelsberger, J.W., Lempicki, R.A., Baseler, M.W., Lane, H.C., 2008. IL-27, a novel anti-HIV cytokine, activates multiple interferon-inducible genes in macrophages. *AIDS* 22, 39–45.
- Kapil, P., Atkinson, R., Ramakrishna, C., Cua, D.J., Bergmann, C.C., Stohlman, S.A., 2009. Interleukin-12 (IL-12), but not IL-23, deficiency ameliorates viral encephalitis without affecting viral control. *J. Virol.* 83 (12), 5978–5986.
- Knobler, R.L., Dubois-Dalcq, M., Haspel, M.V., Claysmith, A.P., Lampert, P.W., Oldstone, M.B., 1981. Selective localization of wild type and mutant mouse hepatitis virus (JHM strain) antigens in CNS tissue by fluorescence, light and electron microscopy. *J. Neuroimmunol.* 1, 81–92.
- Lane, T.E., Liu, M.T., Chen, B.P., Asensio, V.C., Samawi, R.M., Paoletti, A.D., Campbell, I.L., Kunkel, S.L., Fox, H.S., Buchmeier, M.J., 2000. A central role for CD4(+) T cells and RANTES in virus-induced central nervous system inflammation and demyelination. *J. Virol.* 74, 1415–1424.
- Lin, M.T., Stohlman, S.A., Hinton, D.R., 1997. Mouse hepatitis virus is cleared from the central nervous systems of mice lacking perforin-mediated cytotoxicity. *J. Virol.* 71, 383–391.
- Liu, M.T., Chen, B.P., Oertel, P., Buchmeier, M.J., Armstrong, D., Hamilton, T.A., Lane, T.E., 2000. The T cell chemoattractant IFN-inducible protein 10 is essential in host defense against viral-induced neurologic disease. *J. Immunol.* 165, 2327–2330.
- Liu, M.T., Keirstead, H.S., Lane, T.E., 2001. Neutralization of the chemokine CXCL10 reduces inflammatory cell invasion and demyelination and improves neurological function in a viral model of multiple sclerosis. *J. Immunol.* 167, 4091–4097.
- Liu, J.Q., Liu, Z., Zhang, X., Shi, Y., Talebian, F., Carl Jr., J.W., Yu, C., Shi, F.D., Whitacre, C.C., Trgovcich, J., Bai, X.F., 2012. Increased Th17 and regulatory T cell responses in EBV-induced gene 3-deficient mice lead to marginally enhanced development of autoimmune encephalomyelitis. *J. Immunol.* 188, 3099–3106.
- Parra, B., Hinton, D.R., Marten, N.W., Bergmann, C.C., Lin, M.T., Yang, C.S., Stohlman, S.A., 1999. IFN-gamma is required for viral clearance from central nervous system oligodendroglia. *J. Immunol.* 162, 1641–1647.
- Perlman, S.R., Lane, T.E., Buchmeier, M.J., 1999. Coronaviruses: hepatitis, peritonitis, and central nervous system disease. In: Cunningham, M.W., Fujinami, R.S. (Eds.), *Effects of Microbes on the Immune System*. Lippincott Williams & Wilkins, Philadelphia, pp. 331–348.
- Pewe, L., Perlman, S., 2002. Cutting edge: CD8 T cell-mediated demyelination is IFN-gamma dependent in mice infected with a neurotropic coronavirus. *J. Immunol.* 168, 1547–1551.
- Pewe, L., Haring, J., Perlman, S., 2002. CD4 T-cell-mediated demyelination is increased in the absence of gamma interferon in mice infected with mouse hepatitis virus. *J. Virol.* 76, 7329–7333.
- Pflanz, S., Timans, J.C., Cheung, J., Rosales, R., Kanzler, H., Gilbert, J., Hibbert, L., Churakova, T., Travis, M., Vaisberg, E., Blumenschein, W.M., Mattson, J.D., Wagner, J.L., To, W., Zurawski, S., McClanahan, T.K., Gorman, D.M., Bazan, J.F., de Waal Malefyt, R., Rennick, D., Kastelein, R.A., 2002. IL-27, a heterodimeric cytokine composed of EBI3 and p28 protein, induces proliferation of naive CD4(+) T cells. *Immunity* 16, 779–790.
- Pflanz, S., Hibbert, L., Mattson, J., Rosales, R., Vaisberg, E., Bazan, J.F., Phillips, J.H., McClanahan, T.K., de Waal Malefyt, R., Kastelein, R.A., 2004. WSX-1 and glycoprotein 130 constitute a signal-transducing receptor for IL-27. *J. Immunol.* 172, 2225–2231.
- Phares, T.W., Stohlman, S.A., Hwang, M., Min, B., Hinton, D.R., Bergmann, C.C., 2012. CD4 T cells promote CD8 T cell immunity at the priming and effector site during viral encephalitis. *J. Virol.* 86, 2416–2427.
- Siebler, J., Wirtz, S., Frenzel, C., Schuchmann, M., Lohse, A.W., Galle, P.R., Neurath, M.F., 2008. Cutting edge: a key pathogenic role of IL-27 in T cell-mediated hepatitis. *J. Immunol.* 180, 30–33.
- Stiles, L.N., Hardison, J.L., Schaumburg, C.S., Whitman, L.M., Lane, T.E., 2006. T cell antiviral effector function is not dependent on CXCL10 following murine coronavirus infection. *J. Immunol.* 177, 8372–8380.
- Stohlman, S.A., Weiner, L.P., 1981. Chronic central nervous system demyelination in mice after JHM virus infection. *Neurology* 31, 38–44.
- Stohlman, S.A., Bergmann, C.C., Lin, M.T., Cua, D.J., Hinton, D.R., 1998. CTL effector function within the central nervous system requires CD4+ T cells. *J. Immunol.* 160, 2896–2904.
- Stumhofer, J.S., Laurence, A., Wilson, E.H., Huang, E., Tato, C.M., Johnson, L.M., Villarino, A.V., Huang, Q., Yoshimura, A., Sehy, D., Saris, C.J., O’Shea, J.J., Hennighausen, L., Ernst, M., Hunter, C.A., 2006. Interleukin 27 negatively regulates the development of interleukin 17-producing T helper cells during chronic inflammation of the central nervous system. *Nat. Immunol.* 7, 937–945.
- Tong, H., Miyazaki, Y., Yamazaki, M., Hara, H., Waldmann, H., Hori, S., Yoshida, H., 2010. Exacerbation of delayed-type hypersensitivity responses in EBV-induced gene-3 (EBI-3)-deficient mice. *Immunol. Lett.* 128, 108–115.
- Villarino, A., Hibbert, L., Lieberman, L., Wilson, E., Mak, T., Yoshida, H., Kastelein, R.A., Saris, C., Hunter, C.A., 2003. The IL-27R (WSX-1) is required to suppress T cell hyperactivity during infection. *Immunity* 19, 645–655.
- Wojno, E.D., Hunter, C.A., 2012. New directions in the basic and translational biology of interleukin-27. *Trends Immunol.* 33, 91–97.
- Yang, J., Yang, M., Htu, T.M., Ouyang, X., Hanidu, A., Li, X., Sellati, R., Jiang, H., Zhang, S., Li, H., Zhao, J., Ting, A.T., Mayer, L., Unkeless, J.C., Labadia, M.E., Hodge, M., Li, J., Xiong, H., 2008. Epstein-Barr virus-induced gene 3 negatively regulates IL-17, IL-22 and RORgamma t. *Eur. J. Immunol.* 38, 1204–1214.
- Yoshida, H., Miyazaki, Y., 2008. Regulation of immune responses by interleukin-27. *Immunol. Rev.* 226, 234–247.
- Zahn, S., Wirtz, S., Birkenbach, M., Blumberg, R.S., Neurath, M.F., von Stebut, E., 2005. Impaired Th1 responses in mice deficient in Epstein-Barr virus-induced gene 3 and challenged with physiological doses of *Leishmania major*. *Eur. J. Immunol.* 35, 1106–1112.